Simulated 21st century's increase in oceanic suboxia by CO_2-enhanced biotic carbon export

Andreas Oschlies,[1] Kai G. Schulz,[1] Ulf Riebesell,[1] and Andreas Schmittner[2]

[1] The primary impacts of anthropogenic CO_2 emissions on marine biogeochemical cycles predicted so far include ocean acidification, global warming induced shifts in biogeographical provinces, and a possible negative feedback on atmospheric CO_2 levels by CO_2-fertilized biological production. Here we report a new potentially significant impact on the oxygen-minimum zones of the tropical oceans. Using a model of global climate, ocean circulation, and biogeochemical cycling, we extrapolate mesocosm-derived experimental findings of a pCO_2-sensitive increase in biotic carbon-to-nitrogen drawdown to the global ocean. For a simulation run from the onset of the industrial revolution until A.D. 2100 under a "business-as-usual" scenario for anthropogenic CO_2 emissions, our model predicts a negative feedback on atmospheric CO_2 levels, which amounts to 34 Gt C by the end of this century. While this represents a small alteration of the anthropogenic perturbation of the carbon cycle, the model results reveal a dramatic 50% increase in the suboxic water volume by the end of this century in response to the respiration of excess organic carbon formed at higher CO_2 levels. This is a significant expansion of the marine "dead zones" with severe implications not only for all higher life forms but also for oxygen-sensitive nutrient recycling and, hence, for oceanic nutrient inventories.

Citation: Oschlies, A., K. G. Shulz, U. Riebesell, and A. Schmittner (2008), Simulated 21st century's increase in oceanic suboxia by CO_2-enhanced biotic carbon export, *Global Biogeochem. Cycles*, *22*, GB4008, doi:10.1029/2007GB003147.

1. Introduction

[2] A special feature of today's marine oxygen distribution is the presence of extended oxygen-minimum zones in the tropical oceans, with suboxic conditions (here defined by dissolved $O_2 < 5$ mmol m^{-3}) at relatively shallow depths from several tens to hundreds of meters (Figures 1a and 1c). Besides providing a hostile environment for almost all marine life, these regions are of particular biogeochemical relevance because they allow for anaerobic conversion of fixed nitrogen, a major nutrient essential for biological production, into gaseous N_2 not accessible to most organisms. Sediment records provide evidence that the regional patterns of this oxygen-sensitive nutrient loss have varied on millennial and longer timescales in the past, in concert with changes in the extent of the suboxic ocean areas [*Altabet et al.*, 1995, 2002; *Ganeshram et al.*, 2002; *Hendy and Pedersen*, 2006]. Such changes can be driven by variations in biotically controlled local remineralization and associated oxygen consumption or by changes in the physical oxygen supply via circulation and temperature-dependent oxygen solubility.

[3] Modeling studies addressing glacial-interglacial variations have already indicated that the volume of the tropical suboxic areas is highly sensitive to climate change. *Meissner et al.* [2005] showed that purely physical changes in the formation of Antarctic Intermediate Water and North Pacific Intermediate Water, such as associated with glacial-interglacial climate variations, have the potential to reduce the volume of suboxic waters and implied glacial denitrification rates by more than 50% compared to present-day values. A coupled physical-biogeochemical mechanism has been proposed by *Schmittner et al.* [2007] to explain rapid reorganizations of tropical oxygen-minimum zones on centennial timescales via changes in local nutrient supply and biological production driven by remote changes in the North Atlantic overturning circulation.

[4] For the anthropocene, recent measurements and model simulations have identified decreasing concentrations of dissolved oxygen over large regions of the world ocean during the last decades [*Joos et al.*, 2003; *Stramma et al.*, 2008]. In many regions the oxygen decline is several times larger than expected from temperature-related changes in the gas solubility alone and is generally linked to a reduced ventilation of the ocean interior [*Matear et al.*, 2000]. On the basis of an analysis of climate model runs, *Gnanadesikan et al.* [2007] suggested that waters in the tropical thermocline may, in fact, become younger as a result of reduced upwelling of deep waters under global warming scenarios. In the absence of biogeochemical tracers in their analyzed

---

[1]IFM-GEOMAR, Leibniz-Institut für Meereswissenschaften, Kiel, Germany.
[2]College of Oceanic and Atmospheric Sciences, Oregon State University, Corvallis, Oregon, USA.
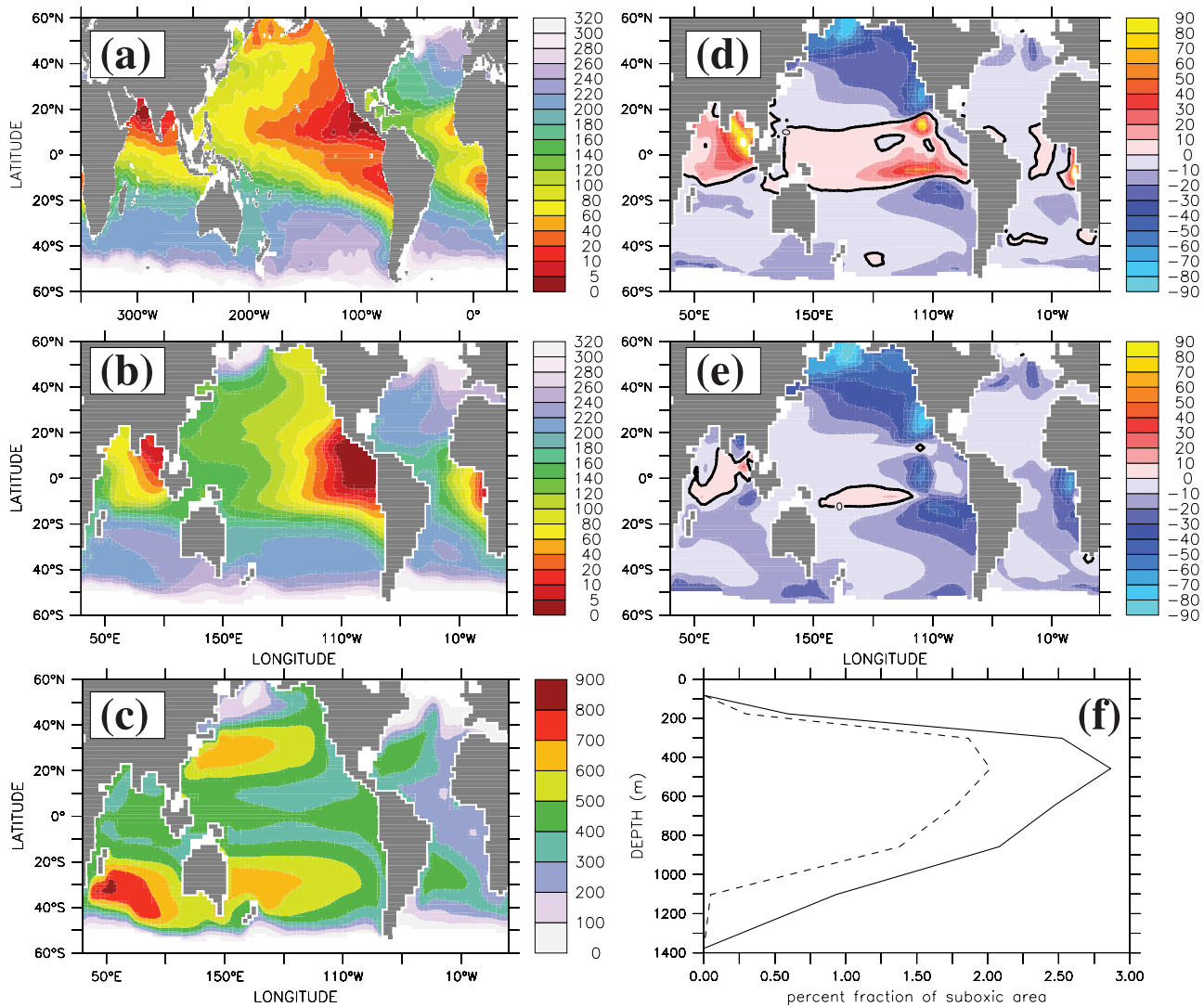
Figure 1. Dissolved oxygen on the $\sigma_0 = 27.0$ kg m^{-3} isopycnal surface. (a) Gridded data taken from *Locarnini et al.* [2002] in mmol m^{-3} and (b) simulated by the model for A.D. 1990. (c) Modeled depth (in meters) of the $\sigma_0 = 27.0$ kg m^{-3} isopycnal surface. (d) Simulated percent change A.D. 2100 minus A.D. 1990 in dissolved oxygen on the same isopycnal for the model with constant elemental stoichiometry and (e) for the model with pCO$_2$-sensitive carbon-to-nitrogen ratios. (f) Percent fraction of simulated A.D. 2100 global suboxic area as a function of depth for pCO$_2$-sensitive carbon-to-nitrogen (C:N) ratios (solid line) and for constant C:N stoichiometry (dashed line).

climate models, they speculated that the reduction in water age might coincide with local increases in dissolved oxygen, contrasting the generally expected decline of the global ocean's oxygen inventory. An increase of oxygen levels in the tropical thermocline was found in the global warming simulations of *Matear and Hirst* [2003], who attributed this to a local reduction in export production in their model. A recent compilation of oxygen measurements taken since the 1960s shows, however, a slight decrease in oxygen levels in the tropical thermocline [*Stramma et al.*, 2008]. While we do not know whether this observed tropical oxygen decrease will extend into the future (and, thus, into the warmer climates analyzed in the above model studies), a possible explanation of this apparent model data discrepancy is that

the complex equatorial current systems which transport oxygen into the tropical oxygen-minimum zones [*Brandt et al.*, 2008] are not adequately represented in coarse-resolution climate models. This caveat is relevant for the present study that also employs a coarse-resolution biogeochemical climate model.

[5] By combining current climate model simulations with empirical models of surface chlorophyll, *Sarmiento et al.* [2004] suggested a modest increase in marine primary production during this century mainly as a result of temperature-related increases in phytoplankton productivity. Globally averaged export production, on the other hand, is predicted to decline by a few percent by the end of the century in response to enhanced stratification and reduced

upwelling of nutrients [*Bopp et al.*, 2001]. Assuming constant elemental stoichiometry that links nitrogen, phosphorus, carbon, and oxygen changes during the formation and degradation of organic particles [*Redfield*, 1934; *Anderson and Sarmiento*, 1994], this will result in reduced oxygen consumption at depth. This biotically induced tendency toward higher oxygen levels is thought to be small compared to the temperature- and circulation-driven oxygen decline [*Bopp et al.*, 2002] with the possible exception of the tropical oceans [*Matear and Hirst*, 2003].

[6] For previous biogeochemical climate change studies that have been based mostly on phosphate as major nutrient, oxygen-sensitive processes like denitrification and anaerobic ammonium oxidation have commonly not been of much concern, and the explicit consideration of such processes could even be avoided. Accordingly, earlier work typically focused on basin-scale to global changes in oxygen inventories rather than on the particular and more regional evolution of the biogeochemically and ecologically distinct oxygen-minimum zones. In the current study, we employ a new biogeochemical model that explicitly resolves the marine nitrogen, phosphorus, carbon, and oxygen cycles [*Schmittner et al.*, 2008]. We use this model to extrapolate recent experimental results that suggest a systematic increase in the carbon-to-nitrogen (C:N) drawdown by biological production [*Riebesell et al.*, 2007] to global and centennial scales. Possible changes in the C:N ratio have already been investigated by *Schneider et al.* [2004] with respect to their potential impact on atmospheric CO_2. They reported a negative feedback on atmospheric CO_2 levels amounting to about 70 Gt C by the end of this century. Although this is nonnegligible with respect to natural variations including glacial-interglacial changes, the feedback is small compared to the total anthropogenic CO_2 emissions that will, according to the Special Report on Emissions Scenarios (SRES) A2 nonintervention scenario, have reached more than 1700 Gt C by A.D. 2100.

[7] While the model we use contains a simple parameterization of calcification as well as calcium carbonate export and dissolution, we explicitly exclude possible acidification-related effects of increasing CO_2 on the calcium carbonate cycle [*Riebesell et al.*, 2000]. To some extent, such effects have already been explored in model studies [e.g., *Heinze*, 2004; *Gehlen et al.*, 2007] and found to generate feedbacks on atmospheric CO_2 considerably smaller than those of the C:N ratio changes investigated by *Schneider et al.* [2004]. In our view, the dramatic effect of changes in the C:N ratio on oxygen levels and in particular on oxygen-minimum zones and oxygen-sensitive nutrient loss processes has not yet been examined. This will be the main focus of the present paper, although feedbacks on atmospheric CO_2 will also be discussed briefly.

2. Methods

[8] The model used is the UVic Earth System Climate Model [*Weaver et al.*, 2001] in the configuration described by *Schmittner et al.* [2008]. The ocean component includes a simple marine ecosystem model with the two major nutrients (nitrate and phosphate) and two phytoplankton

classes (nitrogen fixers and other phytoplankton), thereby allowing for an explicit representation of denitrification and nitrogen fixation. In contrast to other phytoplankton, the model's nitrogen fixers are not limited by nitrate because they are able to fix nitrogen from dissolved N_2, though at lower growth rates than those of the other phytoplankton. The trace nutrient iron is not explicitly included in the model, which nevertheless achieves a reasonable fit to observed biogeochemical tracer distributions for the tuned biological parameters and mixing parameterizations [*Schmittner et al.*, 2005, 2008]. The terrestrial vegetation and carbon cycle component is based on the Hadley Centre's TRIFFID model [*Cox et al.*, 2000].

[9] After a spin-up of more than 10,000 years under preindustrial atmospheric and astronomical boundary conditions, the model was run under historical conditions from A.D. 1765 to 2000 using fossil fuel and land use carbon emissions as well as solar, volcanic, and anthropogenic aerosol forcings [*Schmittner et al.*, 2008]. From A.D. 2000 to 2100, the model was forced by CO_2 emissions following the SRES A2 nonintervention scenario that assumes high population growth and moderate and uneven economic growth, leading to an increase from today's emissions of about 8 Gt C a^{-1} to about 29 Gt C a^{-1} in 2100. In the standard run, we assumed no fertilization effect by enhanced CO_2 levels on the marine biology and used a constant elemental stoichiometry with a molar carbon-to-nitrogen ratio of 6.6 over the entire simulation period. A second experiment extrapolates recent empirical evidence for enhanced carbon-to-nitrogen drawdown in a high-CO_2 world described by *Riebesell et al.* [2007]. From mesocosm enclosures of natural plankton communities under atmospheric CO_2 levels of 350, 700, and 1050 μatm, respectively, a linear relationship between atmospheric CO_2 and the ratio of inorganic carbon drawdown to inorganic nitrogen drawdown was inferred. While the mesocosm experiments revealed a C:N drawdown of 6.0 for 350 μatm CO_2 (7.1 at 700 μatm, 7.9 at 1050 μatm), for the model simulations we rescaled the pCO$_2$-sensitive increase to an assumed preindustrial C:N Redfield ratio of 6.6, resulting in a value of about 8.4 for an atmospheric pCO$_2$ of 850 μatm reached by our simulation at the end of this century (Figure 2a). To test the potential impact of such an enhanced pCO$_2$-sensitive biotic carbon drawdown on global biogeochemical cycles, we here apply this mesocosm-derived relationship to the carbon-to-nitrogen ratio of both the formation and remineralization of particulate organic matter in our global model. Apart from the C:N ratio, both model configurations are identical and start from the same preindustrial initial conditions in A.D. 1765. In particular, we assume that the excess carbon drawn down in the pCO$_2$-sensitive experiment sinks and remineralizes in excess at the same rate as the organic matter in the constant C:N run.

[10] We note that the actual process responsible for the excess carbon export was not monitored during the mesocosm experiments and that our interpretation of the measurements follows *Riebesell et al.* [2007]. At the end of the experiments, there is an excess carbon deficit in the surface layer that cannot be explained by storage in particulate organic carbon, dissolved organic carbon (DOC), or dis-
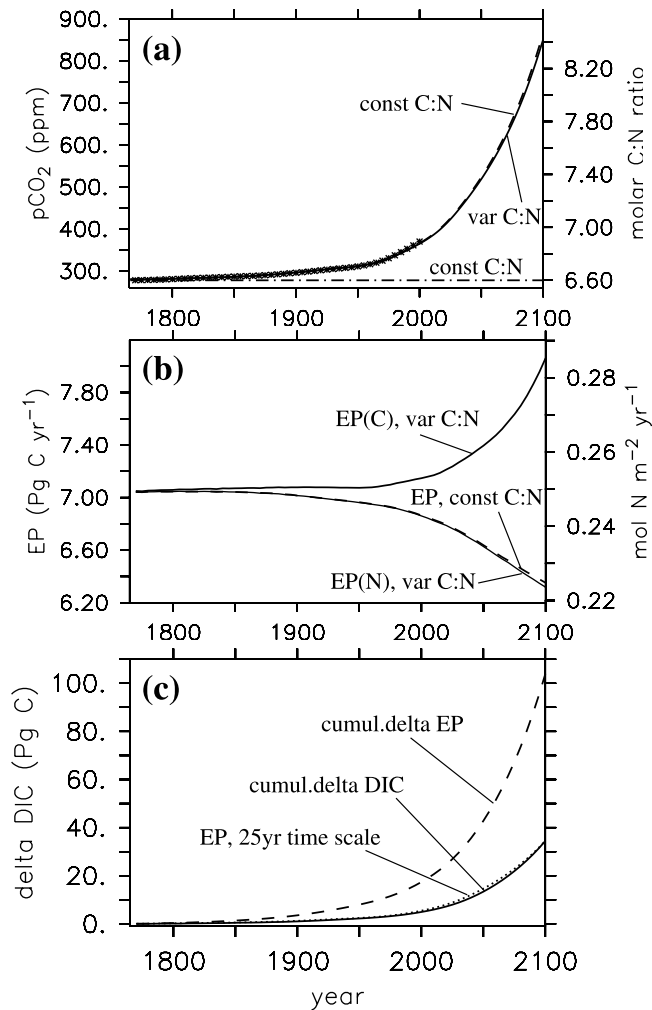
Figure 2. (a) Simulated (solid line) and observed (crosses) annual mean atmospheric pCO_2 (left axis) and corresponding molar carbon-to-nitrogen ratio of the biological pump (right axis). The dashed line just above the solid line refers to the atmospheric pCO_2 (left axis) of the run using constant C:N = 6.6 ratio (dash-dotted line, right axis). The pCO_2-sensitive C:N ratio is inferred from the mesocosm results of *Riebesell et al.* [2007], who performed experiments at 350, 700, and 1050 μatm CO_2 partial pressure. Here, we scaled their results to an assumed preindustrial C:N ratio of 6.6 for 278 μatm (see text). (b) Simulated export production (EP) across z = 125 m. Thick solid line is EP of the pCO_2-sensitive C:N ratio in carbon units (left axis); the thin solid line is in nitrogen units (right axis). The dashed line refers to EP of the constant C:N experiment (left and right axes). (c) Cumulative increase in carbon export of the pCO_2-sensitive experiments compared to the constant C:N experiment (dashed line) and cumulative increase in oceanic dissolved organic carbon inventory (solid line). The dotted line represents the convolution of the increase in export production, $\Delta EP(t) = EP(var.C:N) - EP(const.C:N)$, with a 25 year e-folding decay timescale: $\int_{1765}^{T} \Delta EP(t) e^{(t-T)/25 \text{years}} dt$.

solved inorganic carbon (DIC); by air-sea gas exchange; or by lateral exchange. The only possibility to explain the data is that carbon-rich material has been exported. Since the mesocosms were strongly stratified, we do not see how this export could have happened in the dissolved phase, and we, therefore, postulate an export of particulate matter with a high C:N ratio. As also suggested by *Arrigo* [2007], a likely route is the exudation of DOC and subsequent formation of transparent exopolymer particles (TEP) that could have aggregated with particles, thereby contributing excess carbon to the sinking particle flux.

[11] Acknowledging that we cannot adequately model the (unobserved) mechanism of the excess carbon export, we decided to focus on the fate and biogeochemical impact of the exported matter. Accordingly, we do not attempt to explicitly model DOC or TEP and instead use a simple nutrient-, phytoplankton-, zooplankton-, detritus-type pelagic ecosystem model that simulates a very tight connection between nutrient (and carbon) uptake and export. In a first experiment we used pCO_2-sensitive C:N ratios only for the sinking detritus compartment of the model. This model configuration was, however, not pursued further because of its not very plausible simulation of excess inorganic carbon drawdown during detritus formation rather than during primary production. Instead, we shifted the model's pCO_2-sensitive excess carbon drawdown to primary production which, in the simple model, is equivalent to phytoplankton growth. Accordingly, we simply apply the same pCO_2-sensitive C:N ratios to the formation and remineralization of all of the model's organic matter compartments, i.e., phytoplankton (diazotrophs and other phytoplankton), zooplankton, and detritus. It turned out that annual mean biogeochemical properties simulated by this configuration were very similar to those obtained when pCO_2-sensitive C:N ratios were applied to the detritus compartment only. We note that the mesocosm results reported by *Riebesell et al.* [2007] did not reveal enhanced C:N ratios for the POM suspended in the mixed layer (upper 5.5 m) of the mesocosm. Nevertheless, our model study focuses on the fate of the exported rather than on the suspended material and, to this extent, is fully consistent with the mesocosm data.

[12] We also investigated the impact of expressing the pCO_2 sensitivity of the biotically induced C:N drawdown in terms of the actual pCO_2 of the surface water rather than in terms of pCO_2 of the overlying atmosphere. In contrast to the well-mixed atmosphere, there are substantial regional variations in surface water pCO_2, with high values in the tropical and coastal upwelling regions and lower values in areas of net cooling and deep water formation (Figure 3). Applying the pCO_2-sensitive C:N drawdown derived from the mesocosm experiments to surface water pCO_2 of each grid point column of the model yields C:N ratios ranging, in A.D. 2000, from 6.6 at high latitudes to about 7.5 in the high-pCO_2 upwelling regions in the eastern tropical Pacific, with typical values of 6.9 in the subtropical and tropical oceans. While we are not aware of observational evidence supporting such regional variations in the C:N ratios of carbon-to-nitrogen drawdown, an analysis of sediment trap data did not show significant regional differences in the
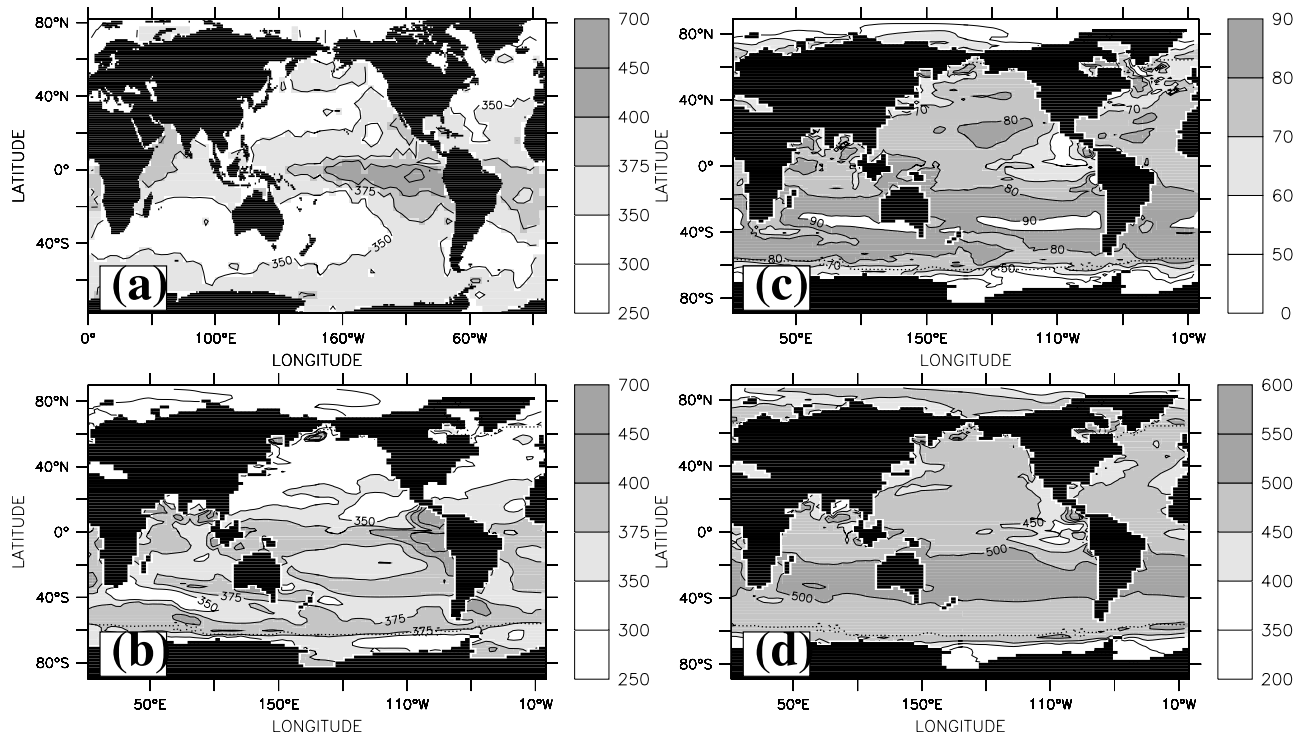
Figure 3. Annual mean surface water pCO_2 as (a) compiled by *Takahashi et al.* [2007] for the reference year 2000 and (b) simulated by the model for A.D. 2000. (c) Simulated increase in surface water pCO_2 during the period 1765−2000 and (d) increase during 2000−2100. Units are μatm. The dotted lines in Figures 3b−3d mark the maximum sea ice extent.

particulate C:N ratios in the upper ocean [(*Schneider et al.*, 2003, Table 4] but may have error bars too large to reliably detect such variations. When pCO_2-sensitive C:N ratios are linked to surface water pCO_2, the regional variability in C:N ratios tends to enhance carbon uptake and export in the high-pCO_2 areas of the tropical oceans and to reduce it at higher latitudes, thereby affecting the mean state of the model. This was accounted for by a new model spin-up over 2000 years under preindustrial conditions before the anthropogenic CO_2 emission experiment was started in year A.D. 1765. Compared to the run relating C:N ratios to atmospheric pCO_2, simulated tropical ocean DIC values are about 2 mmol m^{-3} higher, whereas Arctic Ocean DIC concentrations are up to 5 mmol m^{-3} lower. The effect on simulated dissolved oxygen is a decrease by about 2 mmol m^{-3} in the tropical oceans and an increase by about 2 mmol m^{-3} in the Arctic Ocean. As a consequence of lower tropical oxygen levels, the volume of suboxic waters increases by about 7% with respect to the run relating C:N ratios to atmospheric pCO_2. The resulting increase in denitrification lowers the average nitrate concentrations by less than 1%. These differences are too small to significantly affect model data misfits and, therefore, do not allow for a straightforward assessment of whether using pCO_2-sensitive stoichiometry controlled by surface water pCO_2 improves the model or not.

[13] Despite some differences in the simulated preindustrial steady state, the changes in simulated biogeochemical tracer fields over the period 1765−2100 were essentially insensitive as to whether C:N ratios were related to surface water pCO_2 or to atmospheric pCO_2. This can be attributed to the fact that the simulated increase in surface water pCO_2 is relatively uniform and does not display large regional variability (Figures 3c and 3d). In the following, we, therefore, present only the experiments that use atmospheric pCO_2 to infer the pCO_2-sensitive C:N ratios.

3. Results

[14] The model can well reproduce the observed historical increase in atmospheric CO_2 concentrations from a preindustrial value of 278 to 371 μatm in A.D. 2000 (Figure 2a). Large-scale patterns of physical, biogeochemical, and abiotic transient tracers are also found to be in good agreement with observations, as shown by *Schmittner et al.* [2008]. Simulated annual mean surface water pCO_2 agrees well with observational estimates in the Northern Hemisphere and in the tropical oceans but shows somewhat higher values in the Southern Ocean which, however, has still a relatively poor data coverage (Figure 3). Compared to the gridded oxygen fields from *Locarnini et al.* [2002], our model overestimates the size of the suboxic zones in the equatorial Pacific (Figure 1). This discrepancy can only partly be attributed to the gridding method that likely overestimates minimum oxygen values. Excessive equatorial upwelling of nutrients in our model, a common problem of coarse-resolution circulation models [*Oschlies*, 2000], contributes as well. In the Indian Ocean, lowest simulated
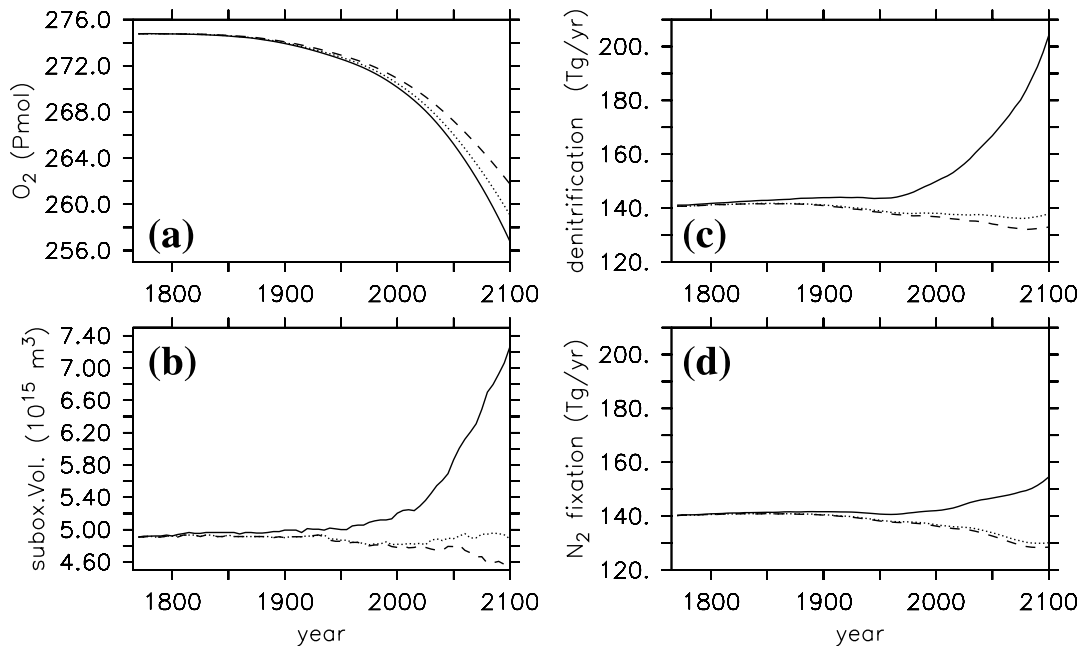
Figure 4. Evolution of (a) the simulated oceanic oxygen inventory and (b) the simulated volume of suboxic waters, here defined by $O_2 < 5$ mmol m^{-3}. (c) Simulated loss of fixed nitrogen by denitrification in Tg N a^{-1} and (d) simulated nitrogen fixation in Tg N a^{-1}. Solid lines refer to the model with pCO$_2$-sensitive carbon-to-nitrogen ratios, dashed lines refer to the model with constant stoichiometry, and dotted lines refer to a sensitivity experiment with C:N ratios kept constant equatorward of 35° latitude and increasing with pCO$_2$ only poleward of 35°. The fact that the dotted lines in Figures 4b, 4c, and 4d are closer to the dashed ones than to the solid ones indicates that on the centennial timescales considered here, changes in the tropical oxygen-minimum zones are relatively insensitive to changes in C:N ratios poleward of 35° latitude.

oxygen values are situated in the Bay of Bengal rather than in the Arabian Sea, similar to other coarse-resolution biogeochemical models [*Moore and Doney*, 2007]. Despite these regional deficiencies that cannot be satisfactorily resolved with our coarse-resolution model, the simulated total oceanic oxygen inventory agrees within 3% with that derived from *Locarnini et al.* [2002]. Simulated global denitrification rates in the water column amount to about 150 Tg N a^{-1} (Figure 4c), which is also in good agreement with recent data-based estimates [*Codispoti*, 2007].

[15] In the control simulation with constant Redfield stoichiometry, global oceanic oxygen levels show a decline in response to increased surface temperatures and an associated reduction in solubility, as well as in response to an increase in stratification and reduced ventilation of deep and intermediate waters (Figure 4a). The decline by about 5% by the end of this century is consistent with the findings of earlier modeling studies employing constant marine stoichiometry [*Matear et al.*, 2000; *Bopp et al.*, 2002]. Counteracting the global trend, there is a slight increase in oxygen concentrations in the upper thermocline in the tropical oceans (Figure 1d). This corresponds to a region for which *Gnanadesikan et al.* [2007] reported a reduction in water mass age in their model, which they attributed to an increase in stratification and reduced mixing with older waters from below. A more detailed investigation of the temporal evolution of tropical oxygen profiles shows that subsurface

oxygen concentrations increase between about 200 and 1200 m depth from A.D. 1765 to A.D. 2100 (Figure 5a). During the same time, δ^{14}C ages decrease, with largest tendency for waters becoming younger at a depth of about 500 m (Figure 5c). In contrast, ventilation is reduced and water ages increase at depths greater than about 2500 m (Figure 5d). These results are qualitatively very similar to those reported by *Gnanadesikan et al.* [2007]. The increase in stratification and associated reduction in upwelling and nutrient supply can also explain the reduction in export production (Figure 6b) which, in turn, is associated with lower oxygen consumption and contributes to the net increase in dissolved oxygen levels in the tropical thermocline for a constant C:N ratio. The modeled volume of suboxic waters shows a corresponding decline by about 7% until A.D. 2100 (Figure 4b). Denitrification and nitrogen fixation also decline by similar percentages (6 and 8% shown in Figures 4c and 4d, respectively). The reduction in denitrification reflects the decrease in both suboxic volume and export production, leaving less organic matter available for denitrification. Nitrogen fixation, in the model, depends on the upwelling of waters with low nitrate-to-phosphate ratios. Because the decline in denitrification leads to elevated nitrate-to-phosphate ratios, this will eventually reduce nitrogen fixation once the oxygen-minimum waters reach the ocean surface.
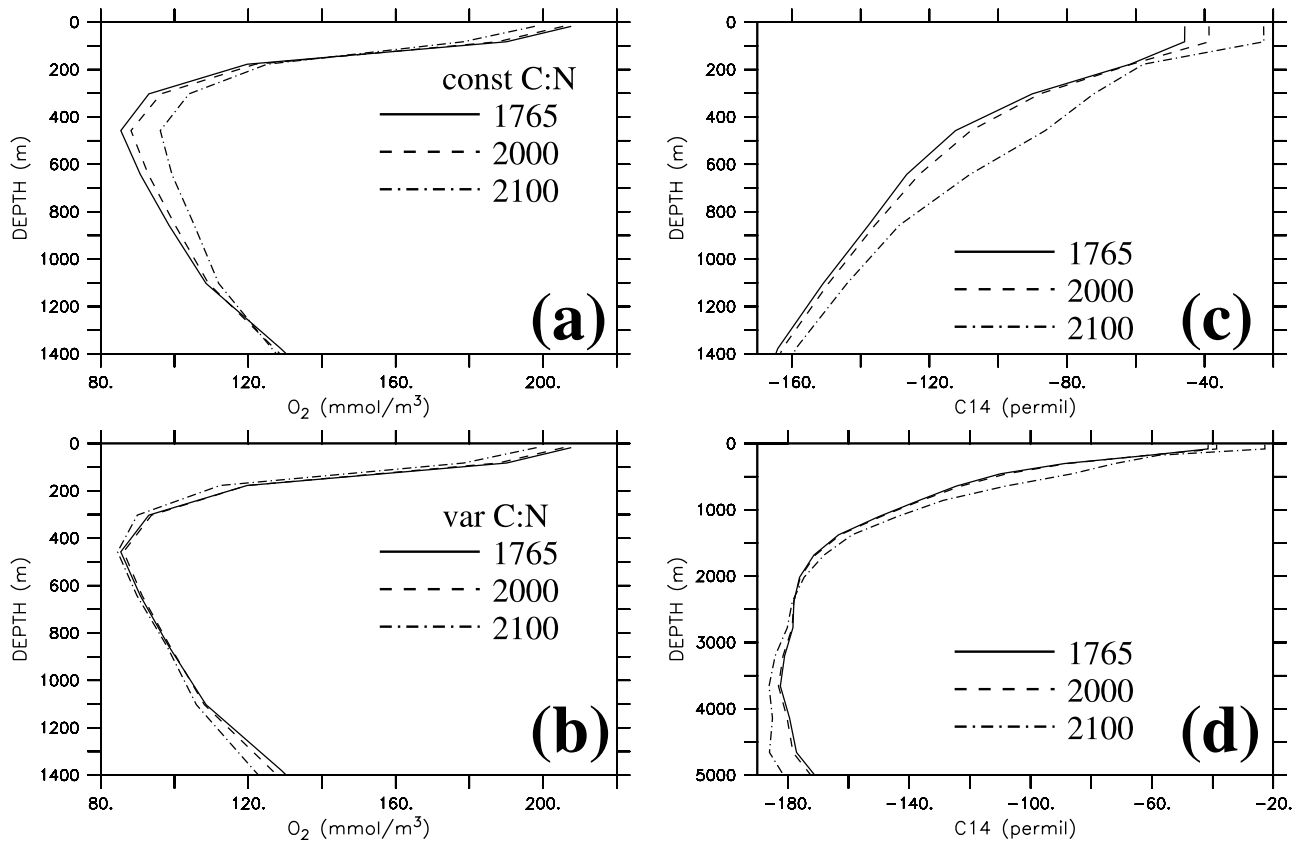
Figure 5. Annual mean profiles of dissolved oxygen (Figures 5a and 5b) and δ^{14}C (Figures 5c and 5d) averaged over the tropical oceans between 10°S and 10°N. (a) Dissolved oxygen simulated by the control run with constant C:N ratios for A.D. 1765 (solid line), 2000 (dashed line), and 2100 (dashed-dotted line). (b) Same as Figure 5a but for the simulation using pCO$_2$-sensitive C:N ratios. Simulated δ^{14}C for (c) the upper 1400 and (d) for the entire depth of the ocean. While Figures 5c and 5d show the run with pCO$_2$-sensitive C:N ratios, the plots are essentially identical for the constant C:N run.

[16] In the simulation with pCO$_2$-sensitive C:N ratios, essentially the same amount of surface nutrient drawdown is associated with an increasingly larger amount of carbon drawdown. This also projects on the simulated carbon and nutrient fluxes exported into the ocean interior (Figures 2b and 6c). Because most of the oxygen consumed during organic matter remineralization is used to oxidize carbon rather than nitrogen, the enhanced C:N ratios then result in excess oxygen consumption at depth. Compared to the constant stoichiometry run, global oxygen levels decrease by another 2% by the end of the century once the pCO$_2$-sensitive description of C:N ratios is included in the model (Figure 4a).

[17] The inclusion of pCO$_2$-sensitive stoichiometry has only limited impact on simulated atmospheric CO$_2$ levels. The enhanced biological carbon drawdown and export lowers atmospheric pCO$_2$ predicted for A.D. 2100 by merely 15 μatm from 866 μatm in the constant C:N run to 851 μatm in the pCO$_2$-sensitive C:N run (Figure 2a). This corresponds to an additional oceanic uptake of 34 Gt C by A.D. 2100 and, thus, represents a negative feedback in the anthropogenically perturbed climate system. While this is significant with respect to natural changes, including glacial-interglacial swings, the magnitude of this feedback effect is small in terms of the anthropogenic perturbation as it amounts to only a few years of current anthropogenic CO$_2$ emissions.

[18] An earlier model study by *Schneider et al.* [2004] employing CO$_2$-dependent C:N ratios for prescribed (rather than prognostic) atmospheric CO$_2$ concentrations reported a somewhat higher additional uptake of anthropogenic CO$_2$ of 70 Gt C by A.D. 2100 for their simulation with increasing C:N ratios. Their higher values can be explained to some extent by their use of particulate C:N ratios increasing with

Figure 6. (a) Simulated preindustrial export production at $z = 125$ m in g C m^{-2} a^{-1}. (b) Difference in export production A.D. 2100 minus A.D. 1765, simulated by the model with constant C:N stoichiometry. (c) Difference in export production A.D. 2100 minus A.D. 1765, simulated by the model with pCO$_2$-sensitive stoichiometry. Units are g C m^{-2} a^{-1}. For both experiments, the corresponding changes in organic nitrogen export follow the pattern of the changes of organic carbon export in the fixed C:N run (Figure 6b, units multiplied by a factor 6.6×12 g C (mol N)$^{-1}$).
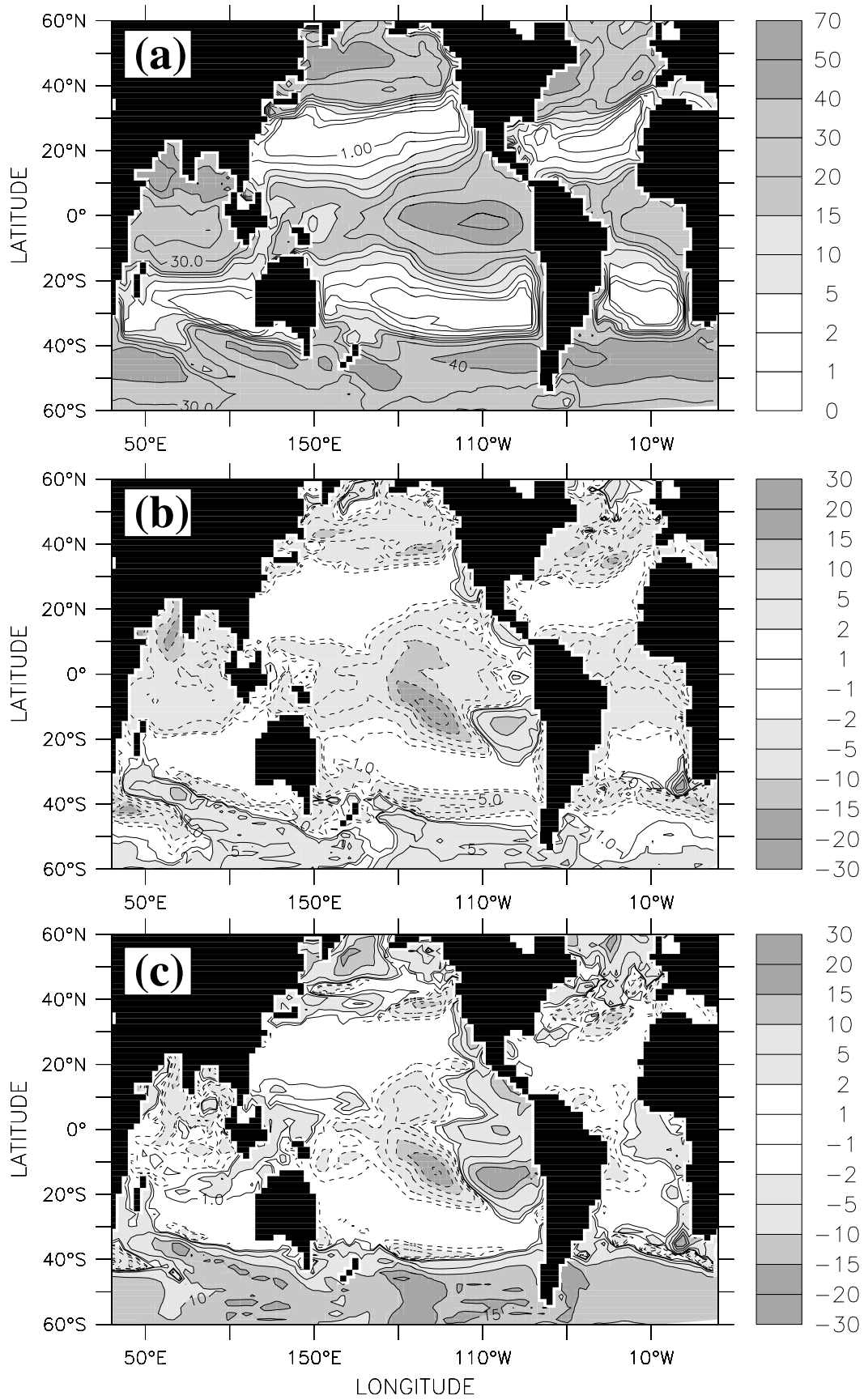
Figure 6

depth. Other factors that contribute to higher sequestration estimates are the neglect of changes in temperature and circulation and the unrealistic implicit assumption of an infinite atmospheric CO_2 reservoir with fixed atmospheric pCO_2, whereas our results reported here use a finite atmospheric box that adjusts its pCO_2 in response to CO_2 fluxes across the air-sea interface.

[19] Note that the additional carbon uptake of 34 Gt C simulated by our model is also much less than the cumulative increase in export production of 104 Gt C by A.D. 2100 (Figure 2c). This difference reflects that most of the additional carbon exported by the biological pump is again in contact with the atmosphere on decadal to centennial timescales [*Oschlies and Kähler*, 2004]. For the current model this can, for the global average, be described by an e-folding timescale of about 25 years (Figure 2c) which is somewhat shorter than typical water ages in the tropical oxygen-minimum zones [*Gnanadesikan et al.*, 2007]. Much of the additional biotically induced carbon uptake occurs in the eastern tropical Pacific (Figure 6c) where the remineralization products can be expected to remain mostly within the warm water sphere and, thus, get in contact with the atmosphere on timescales of decades. Interestingly, the timescale does not change significantly in a sensitivity experiment with variable C:N ratios applied only in regions poleward of 35° latitude. While there is a large amount of additional carbon processed and exported out of the upper 125 m at these higher latitudes (Figure 6c), a substantial portion of this carbon is reentrained into the following winter's deep mixed layers. As long as sinking rates and remineralization profiles are not affected by changing CO_2 levels, our model results suggest that a long-term (>25 years) sequestration of additional carbon by stoichiometric changes in the biological pump is relatively difficult to achieve.

[20] While the impact on atmospheric CO_2 and total oceanic oxygen inventory is small compared to the anthropogenic perturbation, the inclusion of pCO_2-sensitive C:N ratios turns out to generate more dramatic changes in the oxygenation state of the tropical thermocline. Here our model switches from a net oxygen gain under constant Redfield stoichiometry to a net oxygen loss by the end of this century when C:N ratios increase with pCO_2 (Figures 1d and 1e). Relative oxygen losses are largest (up to 70%) near the margins of the suboxic areas where even small changes in oxygen consumption can move oxygen concentrations across the threshold value for suboxia (here 5 mmol m^{-3}). Overall, the volume of suboxic waters increases by about 50% until A.D. 2100 in the model run with pCO_2-sensitive stoichiometry (Figure 4b). As shown by a sensitivity experiment with constant C:N ratios equatorward of 35° latitude and pCO_2-sensitive C:N ratios poleward of 35° (dotted lines in Figure 4), the drastic change in suboxia is, at least until A.D. 2100, essentially a local process caused by changes in carbon export in the tropical oceans.

[21] In concert with the increase in the volume of suboxic waters, simulated denitrification rates increase by more than 40% by the end of this century (Figure 4c) when pCO_2-sensitive C:N ratios are employed. Eventually, these nitrate deficient waters reach the surface and are responsible for the slight decrease in new production and nitrogen-based export production of the pCO_2-sensitive run compared to the experiment with constant C:N ratio (Figure 2b). Since denitrification reduces nitrate-to-phosphate ratios in the suboxic waters of the oxygen-minimum zones, these nitrogen deficit waters may eventually favor nitrogen fixation once they reach the euphotic zone [*Deutsch et al.*, 2007]. While this can provide a stabilizing negative feedback that minimizes changes in the oceanic nitrogen inventory, pathways and transit times needed for oxygen-minimum waters to reach the ocean surface are not currently well known. In our model, simulated nitrogen fixation begins to increase in response to the increase in denitrification within several decades, consistent with denitrification–nitrogen fixation response times in other models [*Moore and Doney*, 2007] (Figure 4d). By the end of this century, simulated nitrogen fixation increases by some 10%, leaving the global ocean's nitrogen budget out of balance with an annual deficit of 50 Tg N.

4. Conclusions

[22] By combining experimental mesocosm data and a global biogeochemical climate model, our study has shown that the tropical oceans and the slowly ventilated oxygen-minimum zones are particularly sensitive to changes in the marine biology. While the standard run with constant Redfield C:N stoichiometry shows an increase in dissolved oxygen levels in the tropical thermocline, the simulation with pCO_2-sensitive C:N drawdown reveals a significant decrease in tropical ocean oxygen concentrations, associated with a 50% increase in the volume of suboxic waters by the end of this century. These large changes in the volume of suboxic waters arise almost entirely from local stoichiometric changes in the tropics. As mesocosm studies investigating the impact of elevated atmospheric CO_2 concentrations on the biological pump have, so far, concentrated on ecosystems at higher latitudes, our extrapolation of these results to the tropics remains speculative and will have to be examined by future experimental studies. Experiments with cultured tropical ocean diazotrophs have already demonstrated a pCO_2-related increase in carbon drawdown very similar to the one inferred from the higher-latitude mesocosm studies used here [*Hutchins et al.*, 2007; *Barcelos e Ramos et al.*, 2007]. We, therefore, do not expect substantial variations in the presumably physiologically driven sensitivity to pCO_2 with latitude. The tropical oceans may also be sensitive to changes in the aeolian supply of the micronutrient iron [*Parekh et al.*, 2006; *Moore and Doney*, 2007]. Although iron-sensitive changes in the biological pump may impact on marine oxygen levels in a way similar to the pCO_2-sensitive C:N changes reported here, this has not explicitly been accounted for in our attempt to isolate and quantify the consequences of a pCO_2-sensitive stoichiometry.

[23] In contrast to the relatively weak negative feedback on atmospheric CO_2, amounting to a few microatmospheres by the end of this century, we find that relatively small changes in the tropical biological pump can have a dramatic impact on the extent of the ecologically and biogeochemically relevant oxygen-minimum zones on surprisingly short

timescales of decades to centuries. Because of the immediate response of oxygen-sensitive losses of fixed nitrogen, the view of a homeostatic nitrogen cycle may not be anymore appropriate as we move from predominantly astronomical to anthropogenic climate forcing in the 21st century.

References

Altabet, M. A., R. Francois, D. W. Murray, and W. L. Prell (1995), Climate-related variations in denitrification in the Arabian Sea from sediment $^{15}N/^{14}N$ ratios, *Nature*, *373*, 506–509.

Altabet, M. A., M. J. Higginson, and D. W. Murray (2002), The effect of millenial-scale changes in Arabian Sea denitrification on atmospheric CO_2, *Nature*, *415*, 159–162.

Anderson, L. A., and J. L. Sarmiento (1994), Redfield ratios of remineralization determined by nutrient data analysis, *Global Biogeochem. Cycles*, *8*, 65–80.

Arrigo, K. R. (2007), Marine manipulations, *Nature*, *450*, 491–492.

Barcelos e Ramos, J., H. Biswas, K. G. Schulz, J. LaRoche, and U. Riebesell (2007), Effect of rising atmospheric carbon dioxide on the marine nitrogen fixer *Trichodesmium*, *Global Biogeochem. Cycles*, *21*, GB2028, doi:10.1029/2006GB002898.

Bopp, L., P. Monfray, O. Aumont, J.-L. Dufresne, H. Le Treut, G. Madec, L. Terray, and J. C. Orr (2001), Potential impact of climate, *Global Biogeochem. Cycles*, *15*, 81–99.

Bopp, L., C. Le Quéré, M. Heimann, A. C. Manning, and P. Monfray (2002), Climate-induced oceanic oxygen fluxes: Implications for the contemporary carbon budget, *Global Biogeochem. Cycles*, *16*(2), 1022, doi:10.1029/2001GB001445.

Brandt, P., V. Hormann, B. Bourlès, J. Fischer, F. A. Schott, L. Stramma, and M. Dengler (2008), Oxygen tongues and zonal currents in the equatorial Atlantic, *J. Geophys. Res.*, *113*, C04012, doi:10.1029/2007JC004435.

Codispoti, L. A. (2007), An oceanic fixed nitrogen sink exceeding 400 Tg N a^{-1} vs. the concept of homeostasis in the fixed-nitrogen inventory, *Biogeosciences*, *4*, 233–253.

Cox, P. M., R. A. Betts, C. D. Jones, S. A. Spall, and I. J. Totterdell (2000), Acceleration of global warming due to carbon-cycle feedbacks in a coupled climate model, *Nature*, *408*, 184–187.

Deutsch, C., J. L. Sarmiento, D. M. Sigman, N. Gruber, and J. P. Dunne (2007), Spatial coupling of nitrogen inputs and losses in the ocean, *Nature*, *445*, 163–167.

Ganeshram, R. S., T. F. Pedersen, S. E. Calvert, and R. François (2002), Reduced nitrogen fixation in the glacial ocean inferred from changes in marine nitrogen and phosphorus inventories, *Nature*, *415*, 156–159.

Gehlen, M., R. Gangstoe, B. Schneider, L. Bopp, O. Aumont, and C. Ethe (2007), The fate of pelagic $CaCO_3$ production in a high CO_2 ocean: A model study, *Biogeosciences*, *4*, 505–519.

Gnanadesikan, A., J. L. Russell, and F. Zang (2007), How does the ocean ventilation change under global warming?, *Ocean Sci.*, *3*, 43–53.

Heinze, C. (2004), Simulating oceanic $CaCO_3$ export production in the greenhouse, *Geophys. Res. Lett.*, *31*, L16308, doi:10.1029/2004GL020613.

Hendy, I. L., and T. F. Pedersen (2006), Oxygen minimum zone expansion in the eastern tropical North Pacific during deglaciation, *Geophys. Res. Lett.*, *33*, L20602, doi:10.1029/2006GL025975.

Hutchins, D. A., F.-X. Fu, Y. Zhang, M. E. Warner, Y. Feng, K. Portune, P. W. Bernhardt, and M. R. Mulholland (2007), CO_2 control of Trichodesmium N2 fixation, photosynthesis, growth rates, and elemental ratios: Implications for past, present, and future ocean biogeochemistry, *Limnol. Oceanogr.*, *52*, 1293–1304.

Joos, F., G.-K. Plattner, T. Stocker, A. Körtzinger, and D. W. R. Wallace (2003), Trends in marine dissolved oxygen: Implications for ocean circulation changes and the carbon budget, *Eos Trans. AGU*, *84*(21), 197,201, doi:10.1029/2003EO210001.

Locarnini, R. A., T. D. O'Brien, H. E. Garcia, J. I. Antonov, T. P. Boyer, M. E. Conkright, and C. Stephens (2002), *World Ocean Atlas 2001*, vol. 3, *Oxygen* [CD-ROM], *NOAA Atlas NESDIS*, vol. 51, NOAA, Silver Spring, Md.

Matear, R. J., and A. C. Hirst (2003), Long-term changes in dissolved oxygen concentration in the ocean caused by protracted global warming, *Global Biogeochem. Cycles*, *17*(4), 1125, doi:10.1029/2002GB001997.

Matear, R. J., A. C. Hirst, and B. I. McNeil (2000), Changes in dissolved oxygen in the Southern Ocean with climate change, *Geochem. Geophys. Geosyst.*, *1*(11), 1050, doi:10.1029/2000GC000086.

Meissner, K. J., E. D. Galbraith, and C. Völker (2005), Denitrification under glacial and interglacial conditions: A physical approach, *Paleoceanography*, *20*, PA3001, doi:10.1029/2004PA001083.

Moore, J. K., and S. C. Doney (2007), Iron availability limits the ocean nitrogen inventory stabilizing feedbacks between marine denitrification and nitrogen fixation, *Global Biogeochem. Cycles*, *21*, GB2001, doi:10.1029/2006GB002762.

Oschlies, A. (2000), Equatorial nutrient trapping in biogeochemical ocean models: The role of advection numerics, *Global Biogeochem. Cycles*, *14*, 655–667.

Oschlies, A., and P. Kähler (2004), Biotic contribution to air-sea fluxes of CO_2 and O_2 and its relation to new production, export production, and net community production, *Global Biogeochem. Cycles*, *18*, GB1015, doi:10.1029/2003GB002094.

Parekh, P., S. Dutkiewicz, M. J. Follows, and T. Ito (2006), Atmospheric carbon dioxide in a less dusty world, *Geophys. Res. Lett.*, *33*, L03610, doi:10.1029/2005GL025098.

Redfield, A. C. (1934), On the proportions of organic derivatives in sea water and their relation to the composition of plankton, in *James Johnstone Memorial Volume*, pp. 176–192, Liverpool Univ. Press, Liverpool, UK.

Riebesell, U., I. Zondervan, B. Rost, P. D. Tortell, R. E. Zeebe, and F. M. M. Morel (2000), Reduced calcification of marine plankton in response to increased atmospheric CO_2, *Nature*, *407*, 364–367.

Riebesell, U., et al. (2007), Enhanced biological carbon consumption in a high CO_2 ocean, *Nature*, *450*, 545–548.

Sarmiento, J. L., et al. (2004), Response of ocean ecosystems to climate warming, *Global Biogeochem. Cycles*, *18*, GB3003, doi:10.1029/2003GB002134.

Schmittner, A., A. Oschlies, X. Giraud, M. Eby, and H. L. Simmons (2005), A global model of the marine ecosystem for long-term simulations: Sensitivity to ocean mixing, buoyancy forcing, particle sinking, and dissolved organic matter cycling, *Global Biogeochem. Cycles*, *19*, GB3004, doi:10.1029/2004GB002283.

Schmittner, A., E. D. Galbraith, S. W. Hostetler, T. F. Pedersen, and R. Zhang (2007), Large fluctuations of dissolved oxygen in the Indian and Pacific oceans during Dansgaard-Oeschger oscillations caused by variations of North Atlantic Deep Water subduction, *Paleoceanography*, *22*, PA3207, doi:10.1029/2006PA001384.

Schmittner, A., A. Oschlies, H. D. Matthews, and E. Galbraith (2008), Future changes in climate, ocean circulation, ecosystems and biogeochemical cycling simulated for a business-as-usual CO_2 emission scenario until year 4000 AD, *Global Biogeochem. Cycles*, *22*, GB1013, doi:10.1029/2007GB002953.

Schneider, B., R. Schlitzer, G. Fischer, and E.-M. Nötig (2003), Depth-dependent elemental composition of particulate organic matter (POM) in the ocean, *Global Biogeochem. Cycles*, *17*(2), 1032, doi:10.1029/2002GB001871.

Schneider, B., A. Engel, and R. Schlitzer (2004), Effects of depth- and CO_2-dependent C:N ratios of particulate organic matter (POM) on the marine carbon cycle, *Global Biogeochem. Cycles*, *18*, GB2015, doi:10.1029/2003GB002184.

Stramma, L., G. C. Johnson, J. Sprintall, and V. Mohrholz (2008), Expanding oxygen-minimum zones in the tropical oceans, *Science*, *320*, 655–658.

Takahashi, T., S. C. Sutherland, and A. Kozyr (2007), Global ocean surface water partial pressure of CO_2 database: Measurements performed during 1968–2006, version 1.0, *Rep. ORNL/CDIAC-152, NDP-088*, 20 pp., Carbon Dioxide Inf. Anal. Cent., Oak Ridge Natl. Lab., Oak Ridge, Tenn.

Weaver, A. J., et al. (2001), The UVic Earth System Climate Model: Model description, climatology, and applications to past, present and future climates, *Atmos. Ocean*, *39*, 361–428.

————————————

A. Oschlies, U. Riebesell, and K. G. Schulz, IFM-GEOMAR, Leibniz-Insitut für Meereswissenschaften, Düsternbrooker Weg 20, D-24105 Kiel, Germany. (aoschlies@ifm-geomar.de; uriebesell@ifm-geomar.de; kschulz@ifm-geomar.de)

A. Schmittner, College of Oceanic and Atmospheric Sciences, Oregon State University, 104 COAS Administration Building, Corvallis, OR 97331-5503, USA. (aschmittner@coas.oregonstate.edu)